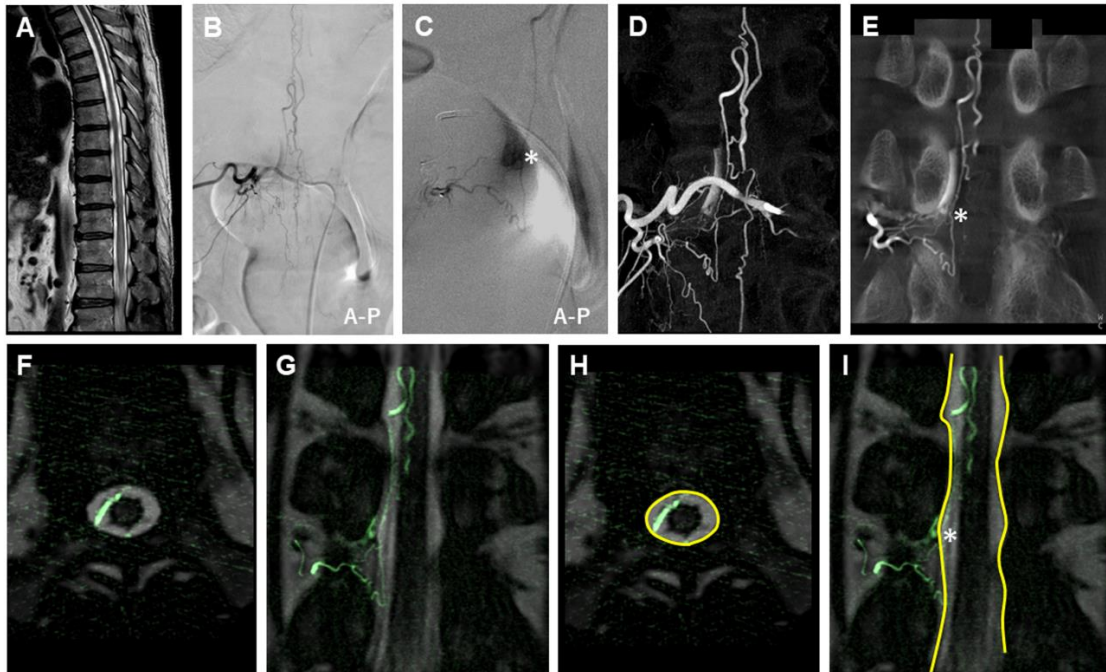
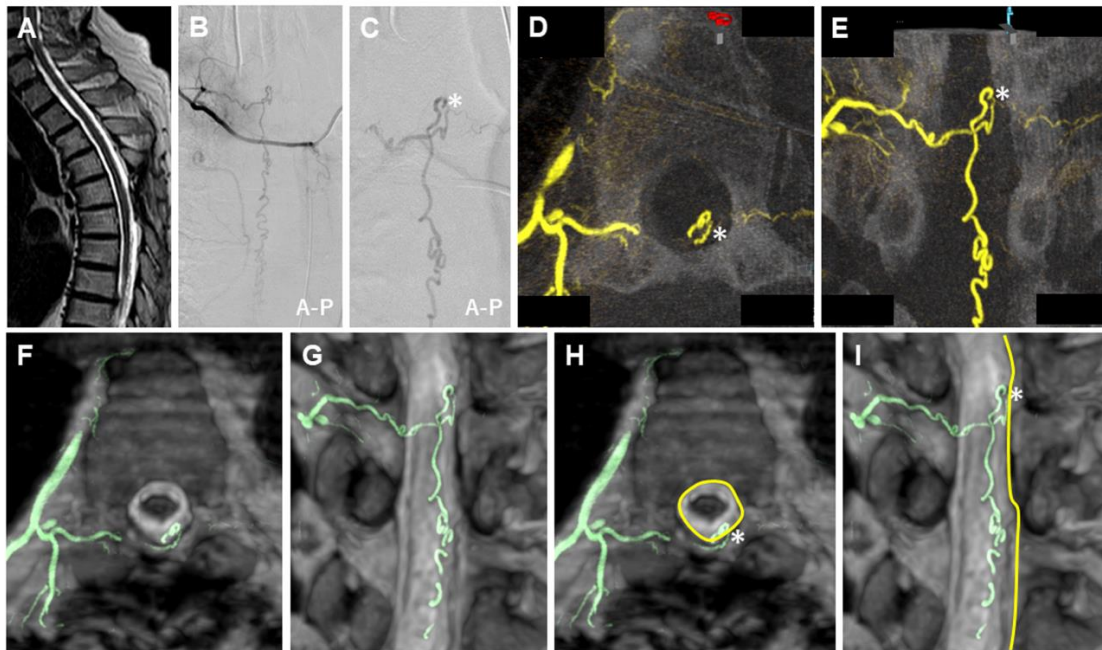


1 **Title of Paper:**2 Diagnostic accuracy of three-dimensional-rotational angiography and heavily T2-weighted
3 volumetric magnetic resonance fusion imaging for the diagnosis of spinal arteriovenous shunts4
5 **Supplementary Figure 1**

6
7 3D-RA/3D-MR fusion images of a SDAVF. Preoperative clinical imaging of a SDAVF in a
8 patient in their 60s. Thoracolumbar sagittal T2-weighted MRI image (A) shows high intensity of
9 the spinal cord. Selective right Th11 segmental artery angiography (B) and selective
10 microcatheter angiography of the feeding artery (C) show an arteriovenous fistula with a single
11 drainage bridging vein into the perimedullary vein supplied by the radiculomeningeal artery. 3D-
12 RA MIP coronal images (D, E) reconstructed from the 3D-RA of the right Th11 segmental artery
13 show the detailed angioarchitecture of the SDAVF. 3D-RA/3D-MR fusion images (slab MIP
14 axial [F] and coronal image [G]) shows the clear 3D relationship with differential contrast
15 between the detailed angioarchitecture of the SDAVF and the surrounding tissue structure,
16 suggesting that the SDAVF shunts into the bridging vein on the dura mater of the spinal
17 nerve root sleeve (F–I). The dura mater is clearly visualized by a black line in contrast to the spinal
18 fluid in the subarachnoid space.
19 The asterisk indicates the shunt point. The yellow line indicates the dura mater of the spinal
20 canal.

1 3D-MR, three-dimensional-heavily T2-weighted volumetric magnetic resonance; 3D-RA, three-
 2 dimensional-rotational angiography; A-P, anterior-posterior; MIP, maximum intensity projection;
 3 MRI, magnetic resonance imaging; SDAVF, spinal dural arteriovenous fistula

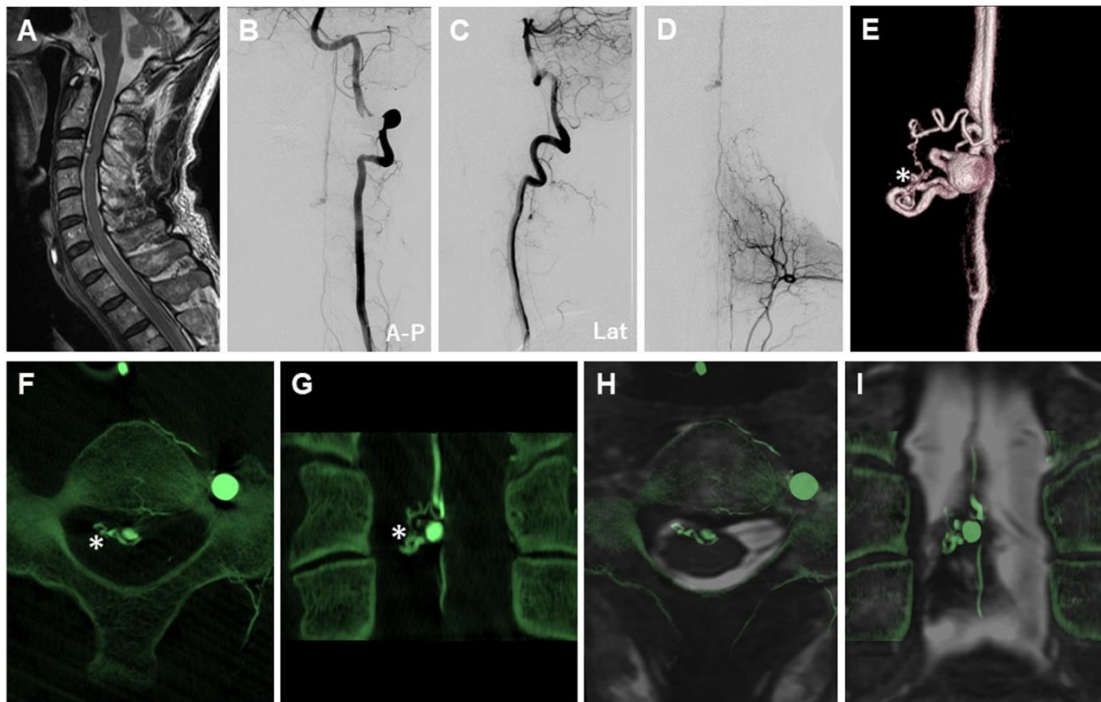
4
 5 **Supplementary Figure 2**



6
 7 3D-RA/3D-MR fusion images of a SDAVF. Preoperative clinical imaging of a SDAVF in a
 8 patient in their 60s. Thoracolumbar sagittal T2-weighted MRI image (A) shows dilated tortuous
 9 vessels around the spinal cord. Selective right Th5 segmental artery angiography (B) and
 10 selective microcatheter angiography of the feeding artery (C) show an arteriovenous fistula with
 11 a single drainage bridging vein into the perimedullary vein supplied by the radiculomeningeal
 12 artery. 3D-RA MIP axial (D) and coronal (E) images reconstructed from the 3D-RA of the right
 13 Th5 segmental artery show the detailed angioarchitecture of the SDAVF. 3D-RA/3D-MR fusion
 14 images (slab MIP axial [F] and coronal image [G]) shows the clear 3D relationship with
 15 differential contrast between the detailed angioarchitecture of the SDAVF and the surrounding
 16 tissue structure, suggesting that the SDAVF shunts into the bridging vein on the dorsal dura
 17 mater of the spinal canal (F–I). The dura mater is clearly visualized by a black line in contrast to
 18 the spinal fluid in the subarachnoid space.
 19 The asterisk indicates the shunt point. The yellow line indicates the dura mater of the spinal
 20 canal.

1 3D-MR, three-dimensional-heavily T2-weighted volumetric magnetic resonance; 3D-RA, three-
 2 dimensional-rotational angiography; A-P, anterior-posterior; MIP, maximum intensity projection;
 3 MRI, magnetic resonance imaging; SDAVF, spinal dural arteriovenous fistula

4
 5 **Supplementary Figure 3.**

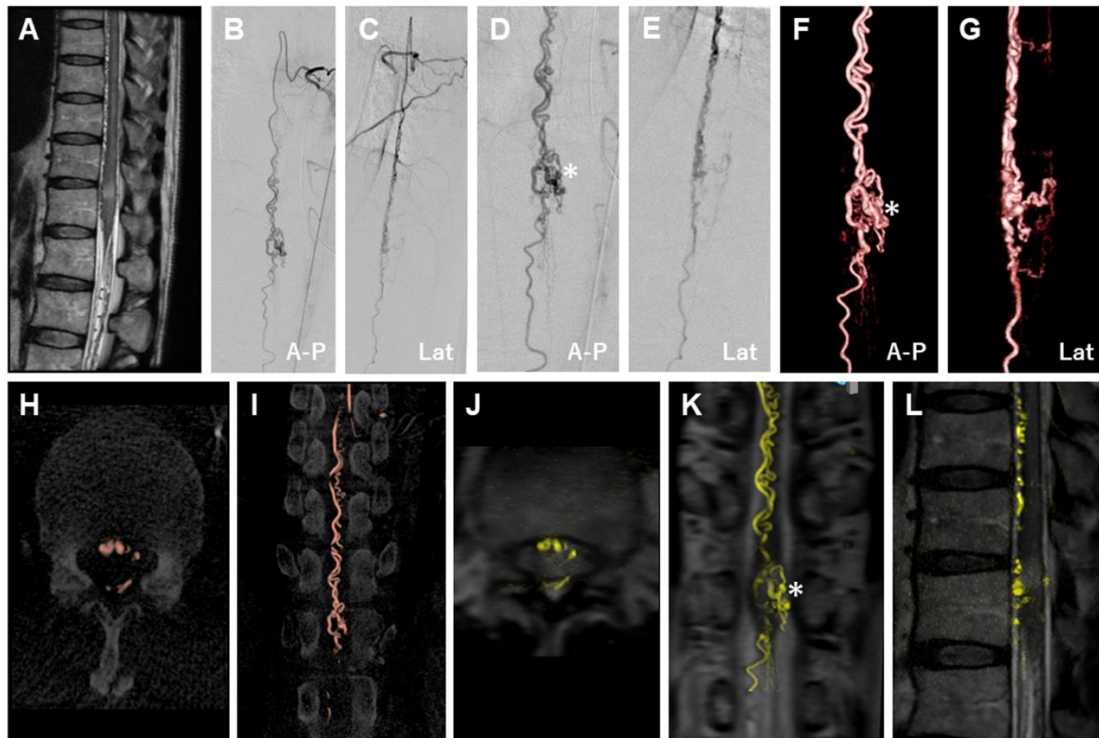


6
 7 3D-RA/3D-MR fusion images of a PMAVF. Preoperative clinical imaging of a PMAVF in a
 8 patient in their 60s. Cervical sagittal T2-weighted MRI image (A) shows varix on the ventral
 9 surface of the cervical spinal cord. Left vertebral artery angiography (B, C), selective left
 10 thyrocervical artery angiography (D) show the spinal AVF with marked dilated varix supplied by
 11 vasocorona from the anterior spinal artery. The volume rendering (E), MIP axial (F), and MIP
 12 coronal (G) images reconstructed from the 3D-RA of the left vertebral artery shows the detailed
 13 angioarchitecture of the AVF. 3D-RA/3D-MR fusion images (slab MIP axial [H] and coronal [I]
 14 image) shows a clear 3D relationship with differential contrast between the detailed
 15 angioarchitecture of the AVF and surrounding tissue structure. The dura mater and spinal cord
 16 are clearly visualized by a black line in contrast to the spinal fluid in the subarachnoid space. The
 17 shunt point is distinctly located on the right lateral surface of the spinal cord, suggesting the
 18 PMAVF with marked dilated varix. The asterisk indicates the shunt point.

1 3D-MR, three-dimensional-heavily T2-weighted volumetric magnetic resonance; 3D-RA, three-
 2 dimensional-rotational angiography; A-P, anterior-posterior; Lat, lateral; MIP, maximum
 3 intensity projection; MRI, magnetic resonance imaging; PMAVF, perimedullary arteriovenous
 4 fistula

5

6 **Supplementary Figure 4.**

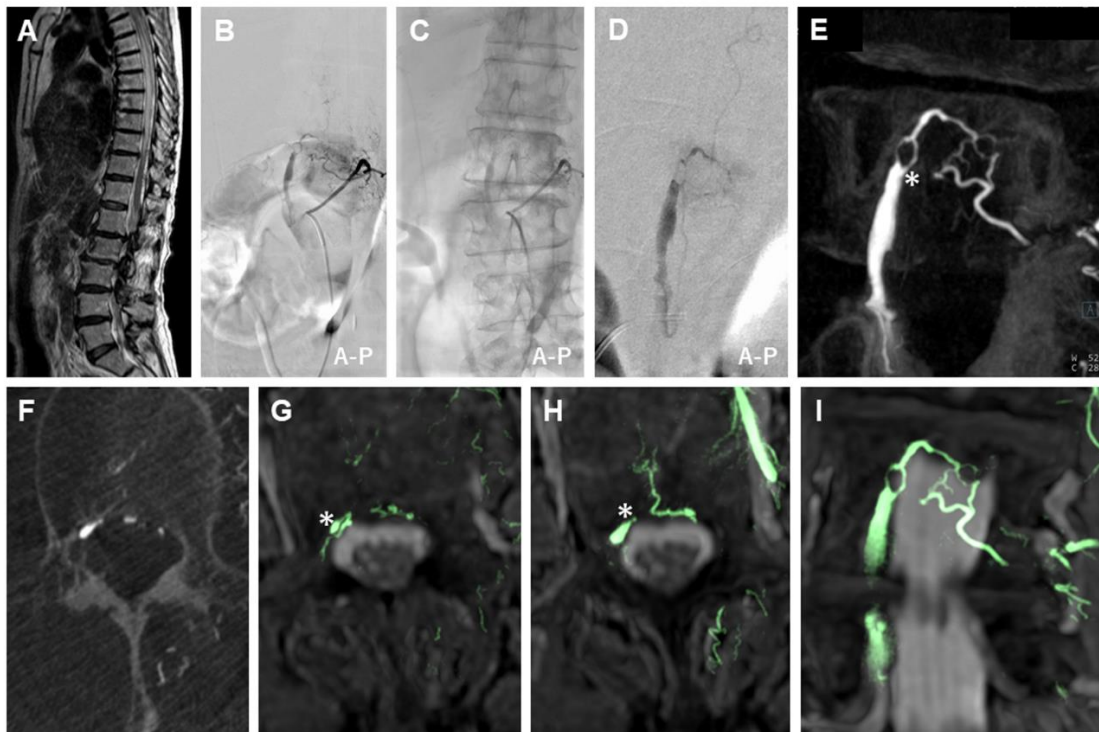


7

8 3D-RA/3D-MR fusion images of a PMAVF. Preoperative clinical imaging of a PMAVF in a
 9 patient in their 60s. Lumbarosacral sagittal T2-weighted MRI image (A) shows high intensity of
 10 the spinal cord at the Th12 level and dilated tortuous vessels around the spinal cord. Left Th8
 11 ASA angiography (B-E) show the spinal AVF with perimedullary venous drainage supplied by
 12 vasacorona from the ASA. The volume rendering (F, G), MIP axial (H), and MIP coronal (I)
 13 images reconstructed from the 3D-RA of the left Th8 ASA shows the detailed angioarchitecture
 14 of the AVF. 3D-RA/3D-MR fusion images (slab MIP axial [J], coronal [K], and sagittal [L]
 15 image) show a clear 3D relationship with differential contrast between the detailed
 16 angioarchitecture of the AVF and surrounding tissue structure. The dura mater and spinal cord
 17 are clearly visualized by a black line in contrast to the spinal fluid in the subarachnoid space. The

1 shunt point is distinctly located on the left lateral surface of the conus medullaris, suggesting the
 2 PMAVF with marked dilated varix. The asterisk indicates the shunt point.
 3 3D-MR, three-dimensional-heavily T2-weighted volumetric magnetic resonance; 3D-RA, three-
 4 dimensional-rotational angiography; A-P, anterior-posterior; ASA, anterior spinal artery; Lat,
 5 lateral; MIP, maximum intensity projection; MRI, magnetic resonance imaging; PMAVF,
 6 perimedullary arteriovenous fistula

7
 8 **Supplementary Figure 5.**



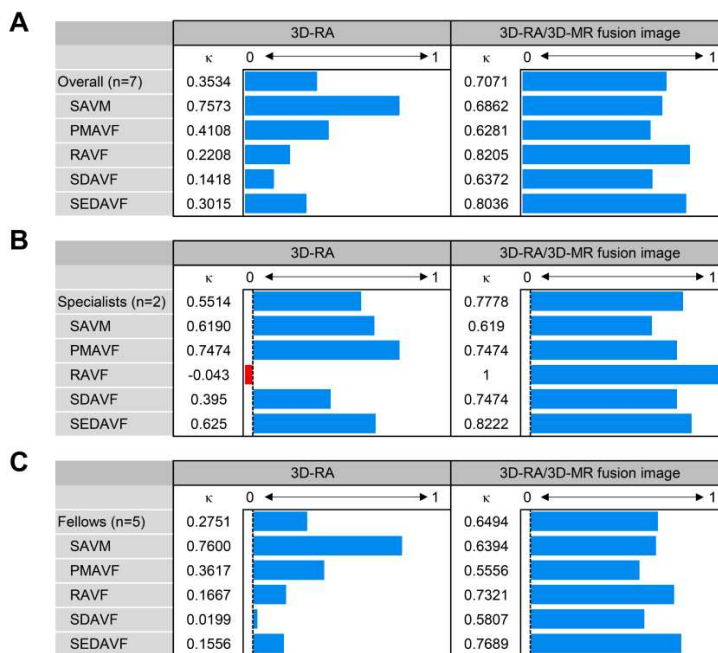
9
 10 3D-RA/3D-MR fusion images of a SEDAVF. Preoperative clinical imaging of a SEDAVF in a
 11 patient in their 70s. Thoracolumbar sagittal T2-weighted MRI image (A) shows high signal
 12 intensity of the spinal cord. Selective left L2 segmental artery angiography (B, C) and selective
 13 microcatheter angiography of the feeding artery (D) show a SEDAVF with an epidural VP
 14 supplied by the left dorsal somatic branch. The AVF drains into the intradural perimedullary vein
 15 through the epidural VP located in the lateral epidural space. MIP coronal (E) and axial (F)
 16 images reconstructed from the 3D-RA of the left L2 segmental artery show the detailed
 17 angioarchitecture of the SEDAVF. 3D-RA/3D-MR fusion images (slab MIP axial [G, H] and
 18 coronal [I] image) shows a clear 3D relationship with differential contrast between the detailed

1 angioarchitecture of the SEAVF and surrounding tissue structure, suggesting that the SEDAVF
 2 shunts into the lateral epidural VP. The dura mater is clearly visualized by a black line in contrast
 3 to the spinal fluid in the subarachnoid space.

4 The asterisk indicates the shunt point.

5 3D-MR, three-dimensional-heavily T2-weighted volumetric magnetic resonance; 3D-RA, three-
 6 dimensional-rotational angiography; A-P, anterior-posterior; MIP, maximum intensity projection;
 7 MRI, magnetic resonance imaging; SEDAVF, spinal epidural arteriovenous fistula; VP, venous
 8 pouch

9
 10 **Supplementary Figure 6.**



11
 12 The interobserver agreements for each diagnostic category of SAVSs. The comparison of the
 13 kappa coefficient between the 3D-RA and 3D-RA/3D-MR fusion images (overall seven
 14 reviewers [A], two specialists [B], and five fellows [C]).

15 3D-MR, three-dimensional-heavily T2-weighted volumetric magnetic resonance; 3D-RA, three-
 16 dimensional-rotational angiography; PMAVF, perimedullary arteriovenous fistula; RAVF,
 17 radicular arteriovenous fistula; SAVM, spinal arteriovenous malformation; SAVS, spinal
 18 arteriovenous shunts; SDAVF, spinal dural arteriovenous fistula; SEDAVF, spinal epidural
 19 arteriovenous fistula; κ , kappa coefficient

20

1 **Supplementary Table 1. Characteristics of patients with spinal arteriovenous shunt**

No.	Age	Diagnosis	Shunt level	Feeder	Symptom
1	70s	SDAVF	Th12	Th12 radiculomenigeal artery	Muscle weakness and sensory disturbance of lower extremities, Bladder dysfunction
2	60s	SEDAVF	Th4	Supreme intercostal artery Th4 segmental artery	Muscle weakness and sensory disturbance of lower extremities, Bladder dysfunction
3	70s	RAVF	C5	C5 and C6 radiculomenigeal artery	Muscle weakness of extremities
4	70s	PMAVF	Th10	Th10 radiculopial artery	Muscle weakness of lower extremities, Bladder dysfunction
5	60s	PMAVF	C3	ASA, Thyrocervical artery	Subarachnoid hemorrhage
6	60s	SDAVF	Th11	Th11 radiculomenigeal artery	Gait disturbance, bladder dysfunction
7	Child	SEDAVF	Th3	Th3 prelaminar artery	Epidural hemorrhage
8	60s	SDAVF	Th5	Th5 radiculomenigeal artery	Gait disturbance
9	70s	SEDAVF	L2	L2 dorsal somatic branch	Gait disturbance, bladder dysfunction
10	50s	PMAVF	Th12 Conus medullaris	Th8 ASA	Sensory disturbance of lower extremities
11	60s	SEDAVF	S2-3	S3 segmental artery	Muscle weakness and sensory disturbance of lower extremities, Bladder dysfunction
12	40s	SAVM	Th12-L1 Conus medullaris	Th10 radiculomedullary artery	Muscle weakness and sensory disturbance of lower extremities

2 ASA, anterior spinal artery; C, cervical; F, female; L, lumbar; M, male; PMAVF, perimedullary arteriovenous fistula; RAVF, radicular arteriovenous
3 fistula; S, sacral; SAVM, spinal cord arteriovenous malformation; SDAVF, spinal dural arteriovenous fistula; SEDAVF, spinal epidural arteriovenous
4 fistula; Th, thoracic